

The 125 GeV Higgs in the context of four generations with 2 Higgs doublets

Michael Geller,^{1,*} Shaouly Bar-Shalom,^{1,†} Gad Eilam,^{1,2,‡} and Amarjit Soni^{3,§}

¹*Physics Department, Technion-Institute of Technology, Haifa 32000, Israel*

²*Center for High Energy Physics, Indian Institute of Science, Bangalore 500 012, India*

³*Theory Group, Brookhaven National Laboratory, Upton, NY 11973, USA*

(Dated: November 27, 2024)

We interpret the recent discovery of a 125 GeV Higgs-like state in the context of a two Higgs doublets model with a heavy 4th sequential generation of fermions, in which one Higgs doublet couples only to the 4th generation fermions, while the second doublet couples to the lighter fermions of the 1st-3rd families. This model is designed to accommodate the apparent heaviness of the 4th generation fermions and to effectively address the low-energy phenomenology of a dynamical electroweak symmetry breaking scenario. The physical Higgs states of the model are, therefore, viewed as composites primarily of the 4th generation fermions. We find that the lightest Higgs, h , is a good candidate for the recently discovered 125 GeV spin-zero particle, when $\tan\beta \sim \mathcal{O}(1)$, for typical 4th generation fermion masses of $M_{4G} = 400 - 600$ GeV, and with a large $t - t'$ mixing in the right-handed quarks sector. This, in turn, leads to $\text{BR}(t' \rightarrow th) \sim \mathcal{O}(1)$, which drastically changes the t' decay pattern. We also find that, based on the current Higgs data, this two Higgs doublet model generically predicts an enhanced production rate (compared to the SM) in the $pp \rightarrow h \rightarrow \tau\tau$ channel and a reduced $VV \rightarrow h \rightarrow \gamma\gamma$ and $p\bar{p}/pp \rightarrow V \rightarrow hV \rightarrow Vbb$ ones. Finally, the heavier CP-even Higgs is excluded by the current data up to $m_H \sim 500$ GeV, while the pseudoscalar state, A , can be as light as 130 GeV. These heavier Higgs states and the expected deviations from the SM in some of the Higgs production channels can be further excluded or discovered with more data.

I. INTRODUCTION

The LHC has recently observed a new scalar particle with a mass around ~ 125 GeV that could be consistent with the Higgs boson of the Standard Model (SM) [1, 2]. In addition, a study of the combined Tevatron data has revealed a smaller broad excess corresponding to a mass between 115 GeV and 135 GeV [3] which is consistent with this LHC discovery. With more data collected, the LHC is expected to be able to unveil the detailed properties of the new scalar particle and verify its nature.

From the theoretical side, there has been a collective effort in the past decades in the search for new physics beyond the SM, that can address some of the fundamental unresolved questions in particle physics. One simple candidate that was extensively studied in the past several years is the so called SM4 (also referred to as “naive” or “simple” SM4); the SM with a fourth sequential generation of fermions (for reviews see [4–7]). This simple extension of the SM was studied for addressing some of the challenges in particle physics, such as: the hierarchy problem [8–11], the origin of matter - anti matter asymmetry in the universe [12, 13] and the apparent anomalies in flavor physics [14–18].

Unfortunately, the recent LHC searches for the SM4 heavy 4th generation quarks have now pushed the exclusion limits to ~ 550 GeV for the t' and ~ 600 GeV for the b' [20], which is on the border of their perturbative

regime. Moreover, the SM4 Higgs was already excluded in the mass range 120 – 600 GeV by the 2011 data [21] when $m_{\nu_4} > m_h/2$. Thus, the above reported discovery of a light Higgs with a mass around 125 GeV is not compatible with the SM4 that includes a heavy 4th generation neutrino with a mass $m_{\nu_4} \gtrsim 100$ GeV, i.e., with a mass larger than the current lower bound on m_{ν_4} [19]. In fact, it was further pointed out recently in [22–25] that the interpretation of the measured Higgs signals is not consistent with the SM4 also for the case $m_{\nu_4} < m_h/2$. In particular, in the SM4, the leading gluon-fusion light Higgs production mechanism is enhanced by a factor of ~ 10 due to the contribution of diagrams with t' and b' in the loops [26], which in general leads to larger signals (than what was observed at the LHC) in the $h \rightarrow ZZ/WW/\tau\tau$ channels. However, if the 4th generation masses are of $\mathcal{O}(600)$ GeV, then the decay channels $h \rightarrow ZZ/WW$ are suppressed due to NLO corrections [27, 28], and the exclusion of the SM4 is based mainly on the $\tau\tau$ channel. In the $h \rightarrow \gamma\gamma$ channel there is also a substantial suppression of $\mathcal{O}(0.1)$ due to (accidental) destructive interference in the loops [26, 29] and another $\mathcal{O}(0.1)$ factor due to NLO corrections [27, 28]. When ν_4 is taken to be light enough so that $\text{Br}(h \rightarrow \nu_4\nu_4)$ becomes $\mathcal{O}(1)$, then the $\gamma\gamma$ channel becomes further suppressed to the level that the observed excess can no longer be accounted for [23]. For a recent comprehensive analysis of the SM4 status in light of the latest Higgs results and electroweak precision data (EWPD), we refer the reader to [30].

However, as was noted already 20 years ago [31] and more recently in [32, 33], if heavy 4th generation fermions are viewed as the agents of electroweak symmetry breaking (and are, therefore, linked to strong dynamics at the nearby TeV-scale), then more Higgs particles are ex-

*Electronic address: mic.geller@gmail.com

†Electronic address: shaouly@physics.technion.ac.il

‡Electronic address: eilam@physics.technion.ac.il

§Electronic address: soni@bnl.gov

pected at the sub-TeV regime. In this case, the Higgs particles may be composites of the 4th generation fermions and the low-energy composite Higgs sector should resemble a two (or more) Higgs doublet framework. Indeed, the phenomenology of multi-Higgs 4th generation models was studied recently in [32–47] and within a SUSY framework in [13, 48–50], for a review see [51]. In [52] it was also shown that the current exclusion limits on the SM4 t' and b' could be significantly relaxed if the four generations scenario is embedded in a 2HDM framework.

Adopting this viewpoint, i.e., that the 4th generation setup should be more adequately described within a multi-Higgs framework, we will study in this paper the expected Higgs signals of a 2HDM with a 4th generation family, investigating whether the interpretation of the recently measured 125 GeV Higgs properties are consistent with one of the neutral scalars of the 4th generation 2HDM.

II. 2HDM'S AND 4TH GENERATION FERMIONS

The 2HDM structure has an inherent freedom of choosing which doublet couples to which fermions. For the three generations 2HDM, three popular setups were suggested which are usually referred to as type I, type II and type III 2HDM. In the case where the 2HDM is assumed to underly some form of TeV-scale strong dynamics mediated by the 4th generation fermions, we expect the Higgs composites to couple differently to the 4th generation fermions. This can be realized in a class of 2HDM models named the 4G2HDM, suggested in [33]. Most of our analysis below is performed in this 4G2HDM framework and a comparison to a 2HDM of type II (which also underlies the SUSY Higgs sector) with and without 4th generations will also be discussed.

Let us recapitulate the salient features of the 2HDM frameworks with a 4th generation of fermions (we will focus below on the quarks sector, but a generalization to the leptonic sector is straight forward). Assuming a common generic 2HDM potential, the phenomenology of 2HDM's is generically encoded in the texture of the Yukawa interaction Lagrangian. The simplest variant of a 2HDM with 4th generations of fermions, can be constructed based on the so called type II 2HDM (which we denote hereafter by 2HDMII), in which one of the Higgs doublets couples only to up-type fermions and the other to down-type ones. This setup ensures the absence of tree-level flavor changing neutral currents (FCNC) and is, therefore, widely favored when confronted with low energy flavor data. The Yukawa terms for the quarks of the 2HDMII, extended to include the extra 4th generation quark doublet is:

$$\mathcal{L}_Y = -\bar{Q}_L \Phi_d F_d d_R - \bar{Q}_L \tilde{\Phi}_u F_u u_R + h.c. , \quad (1)$$

where $f_{L(R)}$ ($f = u, d$) are left(right)-handed fermion fields, Q_L is the left-handed $SU(2)$ quark doublet, F_d, F_u are general 4×4 Yukawa matrices in flavor space and $\Phi_{d,u}$ are the Higgs doublets:

$$\Phi_i = \begin{pmatrix} \phi_i^+ \\ \frac{v_i + \phi_i^0}{\sqrt{2}} \end{pmatrix}, \quad \tilde{\Phi}_i = \begin{pmatrix} \frac{v_i^* + \phi_i^{0*}}{\sqrt{2}} \\ -\phi_i^- \end{pmatrix}. \quad (2)$$

As mentioned above, motivated by the idea that the low energy scalar degrees of freedom may be the composites of the heavy 4th generation fermions, [33] have constructed a new class of 2HDM's, named the 4G2HDM, that can effectively parameterize 4th generation condensation by giving a special status to the 4th family fermions. The possible viable variants of this approach can be parameterized as [33]:

$$\mathcal{L}_Y = -\bar{Q}_L \left(\Phi_\ell F_d \cdot \left(I - \mathcal{I}_d^{\alpha_d \beta_d} \right) + \Phi_h F_d \cdot \mathcal{I}_d^{\alpha_d \beta_d} \right) d_R - \bar{Q}_L \left(\tilde{\Phi}_\ell G_u \cdot \left(I - \mathcal{I}_u^{\alpha_u \beta_u} \right) + \Phi_h G_u \cdot \mathcal{I}_u^{\alpha_u \beta_u} \right) u_R + h.c. , \quad (3)$$

where $\Phi_{\ell,h}$ are the two Higgs doublets, I is the identity matrix and $\mathcal{I}_q^{\alpha_q \beta_q}$ ($q = d, u$) are diagonal 4×4 matrices defined by $\mathcal{I}_q^{\alpha_q \beta_q} \equiv \text{diag}(0, 0, \alpha_q, \beta_q)$.

In particular, in the type I 4G2HDM of [33] (which we will focus on below and which will be denoted hereafter simply as the 4G2HDM), one sets $(\alpha_d, \beta_d, \alpha_u, \beta_u) = (0, 1, 0, 1)$, so that the “heavier” Higgs field (ϕ_h) is as-

sumed to couple only to the 4th generation quarks, while the “lighter” Higgs field (ϕ_ℓ) is responsible for the mass generation of all other (lighter 1st-3rd generations) fermions.

The Yukawa interactions for these 4G2HDM models in terms of the physical states were given in [33]. For the lighter CP-even Higgs it reads:

$$\mathcal{L}(hq_i q_j) = \frac{g}{2m_W} \bar{q}_i \left\{ m_{q_i} \frac{s_\alpha}{c_\beta} \delta_{ij} - \left(\frac{c_\alpha}{s_\beta} + \frac{s_\alpha}{c_\beta} \right) \cdot [m_{q_i} \Sigma_{ij}^q R + m_{q_i} \Sigma_{ji}^{q*} L] \right\} q_j h, \quad (4)$$

$$(5)$$

where α is mixing angle in the CP-even neutral Higgs sector, $\tan \beta = v_h/v_\ell$ is the ratio between the VEVs of Φ_h and Φ_ℓ and Σ^d, Σ^u are new mixing matrices in the down(up)-quark sectors, which are obtained after diagonalizing the quarks mass matrices. These matrices are key parameters of the model, which depend on the rotation (unitary) matrices of the right-handed down and up-quarks, D_R and U_R , and on whether α_q and/or β_q are “turned on”:

$$\begin{aligned} \Sigma_{ij}^d &= \alpha_d D_{R,3i}^* D_{R,3j} + \beta_d D_{R,4i}^* D_{R,4j}, \\ \Sigma_{ij}^u &= \alpha_u U_{R,3i}^* U_{R,3j} + \beta_u U_{R,4i}^* U_{R,4j}. \end{aligned} \quad (6)$$

Thus, as opposed to “standard” 2HDM’s, in the 4G2HDM some elements of D_R and U_R are physical and can, in principle, be measured in Higgs-fermion systems. In particular, inspired by the working assumption of the 4G2HDM and by the observed flavor pattern in the up and down-quark sectors, it was shown in [33] that, for $(\alpha_d, \beta_d, \alpha_u, \beta_u) = (0, 1, 0, 1)$, the new mixing matrices Σ^d and Σ^u are expected to have the following form:

$$\Sigma^u = \begin{pmatrix} 0 & 0 & 0 & 0 \\ 0 & 0 & 0 & 0 \\ 0 & 0 & |\epsilon_t|^2 & \epsilon_t^* \left(1 - \frac{|\epsilon_t|^2}{2}\right) \\ 0 & 0 & \epsilon_t \left(1 - \frac{|\epsilon_t|^2}{2}\right) & \left(1 - \frac{|\epsilon_t|^2}{2}\right) \end{pmatrix}, \quad (7)$$

and similarly for Σ^d by replacing $\epsilon_t \rightarrow \epsilon_b$. The new parameters ϵ_t and ϵ_b are free parameters of the model that effectively control the mixing between the 4th generation and the 3rd generation quarks. We therefore expect $\epsilon_b \ll \epsilon_t$, so that a natural choice for these parameter would be $\epsilon_b \sim \mathcal{O}(m_b/m_{b'})$ and $\epsilon_t \sim \mathcal{O}(m_t/m_{t'})$ (see also [33]). In what follows we will thus set $\epsilon_b = 0$ and vary the $t-t'$ mixing parameter in the range $0 < \epsilon_t < 0.5$.

III. 2HDM’S AND THE 125 GEV HIGGS SIGNALS

Clearly, once a new Higgs doublet is introduced, the phenomenology of the Higgs particles production and decays becomes more complicated. In particular, the new Yukawa couplings depend on several more parameters (i.e., in the 4G2HDM on $\epsilon_t, \epsilon_b, \tan \beta$ and α) and the CP-even Higgs couplings to the W and to the Z bosons have extra pre-factors of $\sin(\alpha - \beta)$ and $\cos(\alpha - \beta)$ (the pseudoscalar A does not couple at tree-level to the W and the Z). As a result, the one-loop $h \rightarrow \gamma\gamma$ decay and the leading $gg \rightarrow h$ Higgs production mechanism can

be significantly altered compared to their SM and SM4 values, depending on $\epsilon_t, \tan \beta, \alpha$ and on the 4th generation fermion masses (i.e., assuming $\epsilon_b \ll \epsilon_t$, therefore setting $\epsilon_b = 0$ throughout our analysis). This is demonstrated in Fig. 1, where we plot the widths $\Gamma(h \rightarrow \gamma\gamma)$ and $\Gamma(h \rightarrow gg)$, as a function of these three parameters setting $M_{4G} \equiv m_{t'} = m_{b'} = m_{l_4} = m_{\nu_4} = 400$ GeV. The dependence on $\tan \beta$ is depicted in a narrow range around $\tan \beta \sim 1$, for which the 4G2HDM is consistent with both EWPD [33] and with the observed 125 GeV Higgs signals (see below).

We see that both $h \rightarrow \gamma\gamma$ and $h \rightarrow gg$ have a strong dependence on the Higgs mixing angle α , while $h \rightarrow \gamma\gamma$ is also very sensitive to $\tan \beta$ and to the new $t-t'$ mixing parameter ϵ_t , due to their role in the interference between the fermion loops and the W-boson loop. In Fig. 2 we further plot the various relevant branching ratios of a 125 GeV h in the 4G2HDM, as a function of α for $\epsilon_t = 0.5, \tan \beta = 1$ and $M_{4G} = 400$ GeV.

Let us now turn to the recently reported LHC Higgs searches and the implications of the discovery of a 125 GeV Higgs-like particle on the 4G2HDM setup with a 4th generation of fermions. The quantity that is usually being used for comparison between the LHC and Tevatron results and the expected signals in various models is the normalized cross-section:

$$R_{XX}^{Model(Obs)} = \frac{\sigma(pp/p\bar{p} \rightarrow h \rightarrow XX)_{Model(Obs)}}{\sigma(pp/p\bar{p} \rightarrow h \rightarrow XX)_{SM}}. \quad (8)$$

For the observed ratios of cross-sections, i.e., the signal strengths R_{XX}^{Obs} , and the corresponding errors σ_{XX} , we use the latest results as published in [1–3]:

- $VV \rightarrow h \rightarrow \gamma\gamma$: 2.2 ± 1.4 (taken from $\gamma\gamma + 2j$)
- $gg \rightarrow h \rightarrow \gamma\gamma$: 1.68 ± 0.42
- $gg \rightarrow h \rightarrow WW^*$: 0.78 ± 0.3
- $gg \rightarrow h \rightarrow ZZ^*$: 0.83 ± 0.3
- $gg \rightarrow h \rightarrow \tau\tau$: 0.2 ± 0.85
- $pp/p\bar{p} \rightarrow hW \rightarrow b\bar{b}W$: 1.8 ± 1.5

The values given above are the result of a combination of the most recent data in each channel.^[1] The uncertainties are calculated by treating the reported experimental

[1] We combine the results from the CMS and ATLAS experiments (for $pp/p\bar{p} \rightarrow hW \rightarrow b\bar{b}W$ we combine the results from CMS and Tevatron), where in cases where the measured value was not explicitly given we estimate it from the published plots.

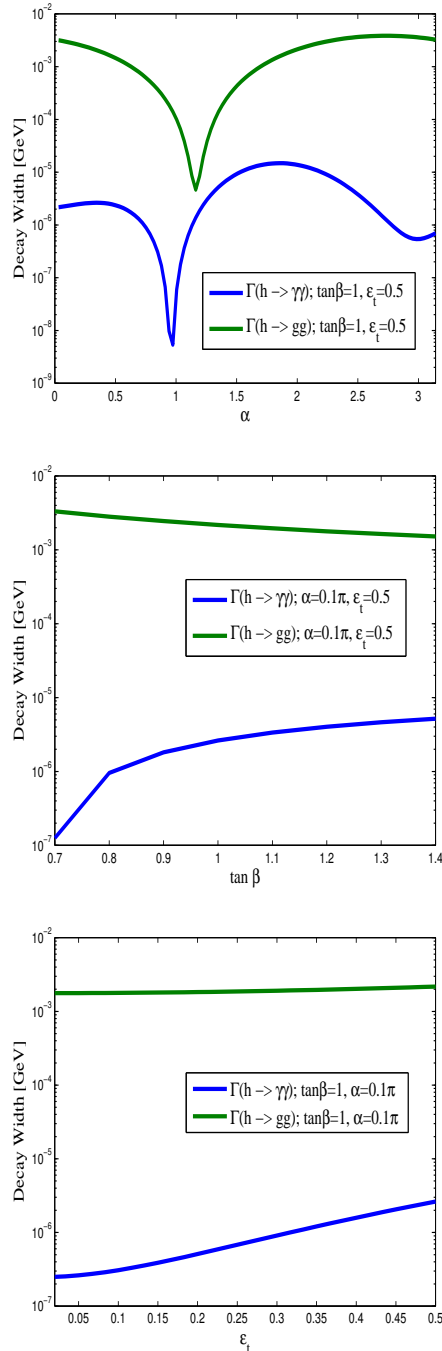


FIG. 1: $\Gamma(h \rightarrow \gamma\gamma)$ and $\Gamma(h \rightarrow gg)$, as a function of α , $\tan\beta$ and ϵ_t , for some representative values of these parameters (as indicated in the plots) and with $M_{4G} \equiv m_{t'} = m_{b'} = m_{l_4} = m_{\nu_4} = 400 \text{ GeV}$.

uncertainties as statistical and assigning 15% theoretical uncertainty to the gluon fusion production mechanism and 5% theoretical uncertainty on electroweak production mechanisms and on the branching fractions [53]. One can easily notice that the channels which have the highest sensitivity to the Higgs signals and contributed the most to the recent 125 GeV Higgs discovery are

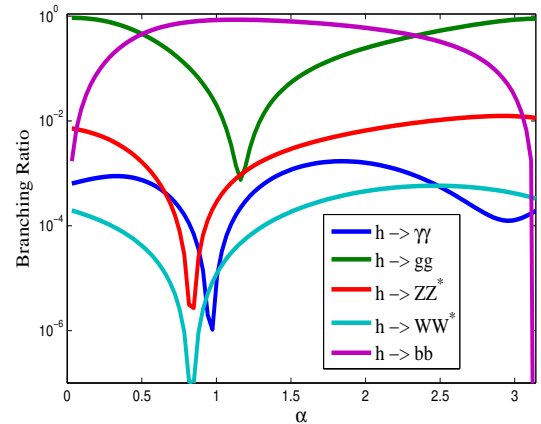


FIG. 2: The relevant branching ratios of h in the 4G2HDM, as a function of α , with $m_h = 125 \text{ GeV}$, $M_{4G} = 400 \text{ GeV}$, $\epsilon_t = 0.5$ and $\tan\beta = 1$.

$h \rightarrow \gamma\gamma$ and $h \rightarrow ZZ^*, WW^*$. In all other channels the results are not conclusive and at this time they are consistent with the background only hypothesis at the level of less than 2σ .

Clearly, a SM Higgs is ideally most consistent with $R_{XX}^{Obs} = 1$ in every channel, while in other models we expect some deviations in the various measured channels, depending on the parameters of the model and on the mass of the scalar candidate which should be compatible with the LHC results. Thus, the comparison to any given model can be performed using a χ^2 fit:

$$\chi^2 = \sum_X \frac{(R_{XX}^{Model} - R_{XX}^{Obs})^2}{\sigma_{XX}^2}, \quad (9)$$

where σ_{XX} are the errors on the observed cross-sections and R_{XX}^{Model} is the calculated normalized cross-section in any given model. In particular, we take advantage of the fact that $\frac{\sigma(Y Y \rightarrow h)_{Model}}{\sigma(Y Y \rightarrow h)_{SM}} = \frac{\Gamma(h \rightarrow Y Y)_{Model}}{\Gamma(h \rightarrow Y Y)_{SM}}$, and calculate R_{XX}^{Model} using

$$R_{XX}^{Model} = \frac{\Gamma(h \rightarrow Y Y)_{Model}}{\Gamma(h \rightarrow Y Y)_{SM}} \cdot \frac{Br(h \rightarrow X X)_{Model}}{Br(h \rightarrow X X)_{SM}}, \quad (10)$$

where $Y Y \rightarrow h$ is the Higgs production mechanism, i.e., either by gluon fusion $g g \rightarrow h$, vector boson fusion $W W / Z Z \rightarrow h$ or the associated Higgs-W production $W^* \rightarrow h W$ at the Tevatron.

The Higgs signals in a 2HDM setup with a 4th generation of fermions have already been discussed to some extent in the literature [43, 44, 46, 47, 55], but with no general picture of how these signals match all the observed Higgs cross-sections reported above. Here, we try to quantify how well the 2HDM scenarios (where the lightest Higgs particle, h , has a mass of 125 GeV) fit all the available Higgs data, by calculating the χ^2 for all the relevant channels in two 2HDM realizations with four generations - the 2HDMII and the 4G2HDM (see section II).

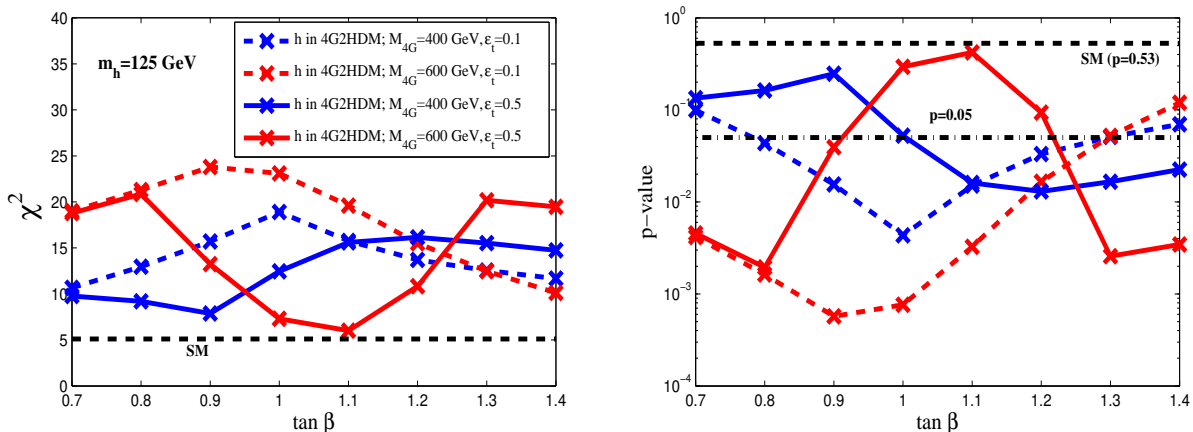


FIG. 3: χ^2 (left plot) and p -values (right plot), as a function of $\tan \beta$, for the lightest 4G2HDM CP-even scalar h , with $m_h = 125$ GeV, $\epsilon_t = 0.1$ and 0.5 and $M_{4G} \equiv m_{t'} = m_{b'} = m_{l_4} = m_{\nu_4} = 400$ and 600 GeV. The value of the Higgs mixing angle α is the one which minimizes χ^2 for each value of $\tan \beta$. The SM best fit is shown by the horizontal dashed-line and the dash-dotted line in the right plot corresponds to $p = 0.05$ and serves as a reference line.

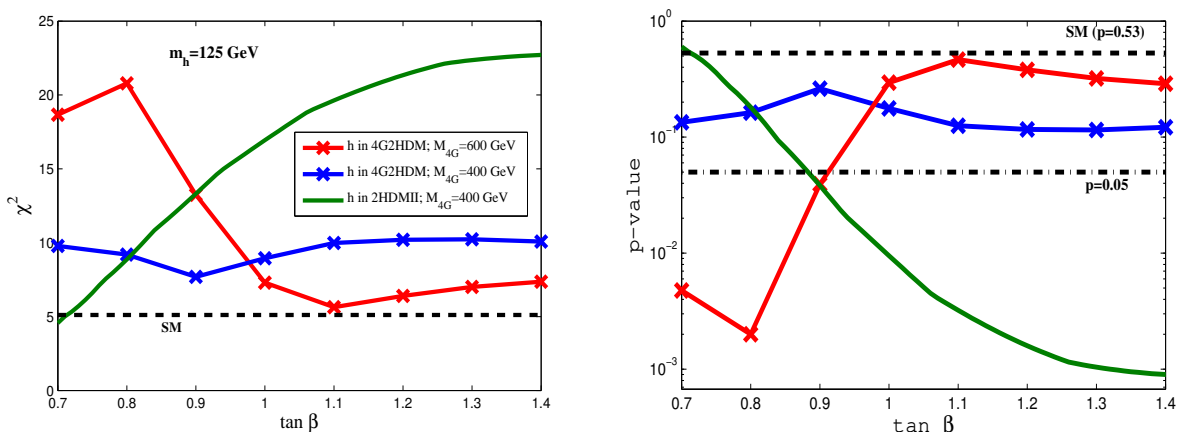


FIG. 4: Same as Figure 3, where here we minimize with respect to both ϵ_t and α for each value of $\tan \beta$. Also shown are the χ^2 and p -values for a 125 GeV Higgs in the SM and in the type II 2HDM with a 4th generation of fermions (denoted by 2HDMII).

We use the latest version of Hdecay [54], with recent NLO contributions which also include the heavy 4th generation fermions, where we have inserted all the relevant couplings of the 4G2HDM and the 2HDMII frameworks described in section II. For the 4th generation fermion masses involved in the loops of the decays $h \rightarrow VV$ (i.e., in the 1-loop NLO corrections for the cases $h \rightarrow ZZ^*, WW^*$), we have used the approximation of a degenerate 4th generation fermion sector, where we have tested below two representative cases: $m_{t'} = m_{b'} = m_{l_4} = m_{\nu_4} \equiv M_{4G} = 400$ and 600 GeV (the effect of mass splittings between 4th generation fermions on $\Gamma(h \rightarrow VV)$ is negligible). It is important to note that, while the first case ($M_{4G} = 400$ GeV) is excluded for the SM4 [20], it is not necessarily excluded for the 4G2HDM, since in this model the decay patterns of t' and b' can have a completely different topology, e.g., having $BR(t' \rightarrow th) \sim 1$, for which the current limits (which are based on the “standard” SM4 decays $t' \rightarrow bW$ and

$b' \rightarrow tW$) do not apply, see [52].

As mentioned earlier, we find that the simple SM4 case, with a 125 GeV Higgs is excluded to many σ 's when confronted with the Higgs search results. Also, as was already noted in [44] in the context of the “standard” 2HDMII (i.e., with four generations), we find that the simplest case of a light 125 GeV pseudoscalar A of any 2HDM, with and without a 4th family, is not compatible with the Higgs data, irrespective of the 4th generation fermion masses. In particular, the signals of the 125 GeV Higgs decaying into a pair of vector bosons, $h \rightarrow ZZ$ and $h \rightarrow WW$, excludes this possibility due to the absence of tree-level AZZ and AWW couplings. We, therefore, focus below only on the case where the observed 125 GeV Higgs-like particle is the lighter CP-even Higgs, h .

We plot in Fig. 3 the resulting χ^2 and p -values in the 4G2HDM case (combining all the six reported Higgs decay channels above), with $m_h = 125$ GeV, $M_{4G} = 400$ and 600 GeV, $\epsilon_t = 0.1$ and 0.5 and for $0.7 < \tan \beta < 1.4$

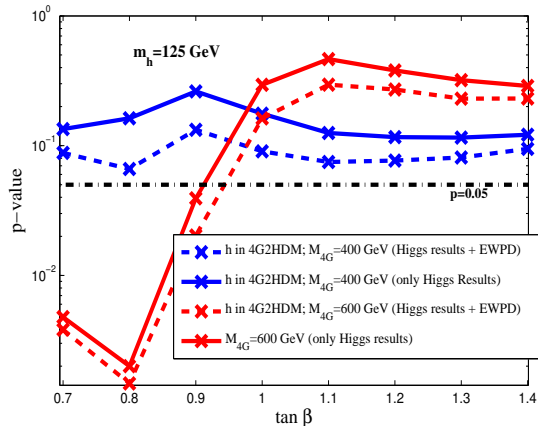


FIG. 5: A comparison between the p -values for the compatibility of the 125 GeV h of the 4G2HDM with the Higgs search results, with (dashed lines) and without (solid lines) imposing the constraints from EWPD as given in [33, 51]. The dash-dotted line corresponds to $p = 0.05$. Here also, the parameters α and ϵ_t are chosen by a minimization of the χ^2 .

(this range is allowed by EWPD and flavor physics in the 2HDM 4th generation setups, see [33, 51]). The value of the Higgs mixing angle α is the one which minimizes the χ^2 for each value of $\tan\beta$. The SM best fit is also shown in the plot. In Fig. 4 we further plot the resulting χ^2 and p -values as a function of $\tan\beta$, this time minimizing for each value of $\tan\beta$ with respect to both α and ϵ_t (in the 4G2HDM case). For comparison, we also show in Fig. 4 the χ^2 and p -values for a 125 GeV h in the 2HDMII with a 4th generation and in the SM.

Looking at the p -values in Figs. 3 and 4 (which “measure” the extent to which a given model can be successfully used to interpret the Higgs data in all the measured decay channels) we see that, h of the 4G2HDM with $\tan\beta \sim \mathcal{O}(1)$ and $M_{4G} = 400 - 600$ GeV is a good candidate for the recently observed 125 GeV Higgs, giving a fit comparable to the SM fit. The “standard” 2HDMII setup with $M_{4G} = 400$ GeV is also found to be consistent with the Higgs data in a narrower range of $\tan\beta \lesssim 0.9$. We find that the fit favors a large $t - t'$ mixing parameter ϵ_t , implying $\text{BR}(t' \rightarrow th) \sim \mathcal{O}(1)$ which completely changes the t' decay pattern [33] and, therefore, significantly relaxing the current bounds on $m_{t'}$ [52]. This can be seen in Table I where we list 6 representative sets of best fitted values (to be used in the plots below) for $\{\tan\beta, \alpha, \epsilon_t, M_{4G}\}$ in the 4G2HDM, that correspond to points on the best fitted 4G2HDM curves shown in Fig. 4.

In Fig. 5 we further test the goodness of fit for the 125 GeV h of the 4G2HDM, where, in addition to the Higgs results, we explicitly imposed the constraints on the 4G2HDM parameter space from EWPD (from the S and T parameters and from $Z \rightarrow b\bar{b}$) using the results in [33, 51]. Evidently, our conclusions above do not change after adding the EWPD constraints to the analysis.

Finally, we note that we have also tested the 3 generations type II 2HDM and found that its lightest CP-even

Higgs is also a good candidate for the observed 125 GeV Higgs particle, giving a fit which is also comparable to the SM fit for $\tan\beta \sim \mathcal{O}(1)$.

| Point # | $ \tan\beta $ | α | ϵ_t | M_{4G} [GeV] |
|---------|---------------|-----------|--------------|----------------|
| P1 | 0.7 | 0.09π | 0.5 | 400 |
| P2 | 0.7 | 0.51π | 0.433 | 600 |
| P3 | 1.0 | 0.1π | 0.42 | 400 |
| P4 | 1.0 | 0.08π | 0.5 | 600 |
| P5 | 1.3 | 0.11π | 0.3 | 400 |
| P6 | 1.3 | 0.07π | 0.33 | 600 |

TABLE I: Six representative best fitted sets of values for $\{\tan\beta, \alpha, \epsilon_t, M_{4G}\}$ in the 4G2HDM, corresponding to points on the best fitted 4G2HDM curves shown in Fig. 4.

IV. HIGGS PHENOMENOLOGY IN THE 4G2HDM

In Fig. 6 we plot the individual pulls and the signal strengths for the various measured channels, $(R_{XX}^{4G2HDM} - R_{XX}^{Obs})/\sigma_{XX}$ and R_{XX}^{4G2HDM} , respectively, as a function of $\tan\beta$, for the above best fitted 4G2HDM curve with $M_{4G} = 400$ GeV. We see that appreciable deviations from the SM are expected in the channels $gg \rightarrow h \rightarrow \tau\tau$, $VV \rightarrow h \rightarrow \gamma\gamma$ and $hV \rightarrow bbV$. In particular, the most notable effects are about a 1.5σ deviation (from the observed value) in the VBF diphoton channel $VV \rightarrow h \rightarrow \gamma\gamma$ and a $2 - 2.5\sigma$ deviation in the $gg \rightarrow h \rightarrow \tau\tau$ channel. The deviations in these channels are in fact a prediction of the 4G2HDM strictly based on the current Higgs data, which could play a crucial role as data with higher statistics becomes available. They can be understood as follows: the channels that dominate the fit (i.e., having a higher statistical significance due to their smaller errors) are $gg \rightarrow h \rightarrow \gamma\gamma, ZZ^*, WW^*$. Thus, since the $gg \rightarrow h$ production vertex is generically enhanced by the t', b' loops, the fit then searches for values of the relevant 4G2HDM parameters which decrease the $h \rightarrow \gamma\gamma, ZZ^*, WW^*$ decays in the appropriate amount. This in turn leads to an enhanced $gg \rightarrow h \rightarrow \tau\tau$ (i.e., due to the enhancement in the $gg \rightarrow h$ production vertex) and to a decrease in the $VV \rightarrow h \rightarrow \gamma\gamma$ and $p\bar{p}/pp \rightarrow W \rightarrow hW \rightarrow bbW$, which are independent of the enhanced ggh vertex but are sensitive to the decreased VVh one. It is important to note that some of the characteristics of these “predictions” can change with more data collected.

We conclude with the implications of the above results for the other two neutral scalars of the 4G2HDM. For the heavier CP-even neutral Higgs, H , we consider its decays to ZZ and WW , which are currently the most sensitive channels in which searches for a heavy SM Higgs were performed at the LHC. A useful approximation of the expected exclusion range on m_H can be performed by

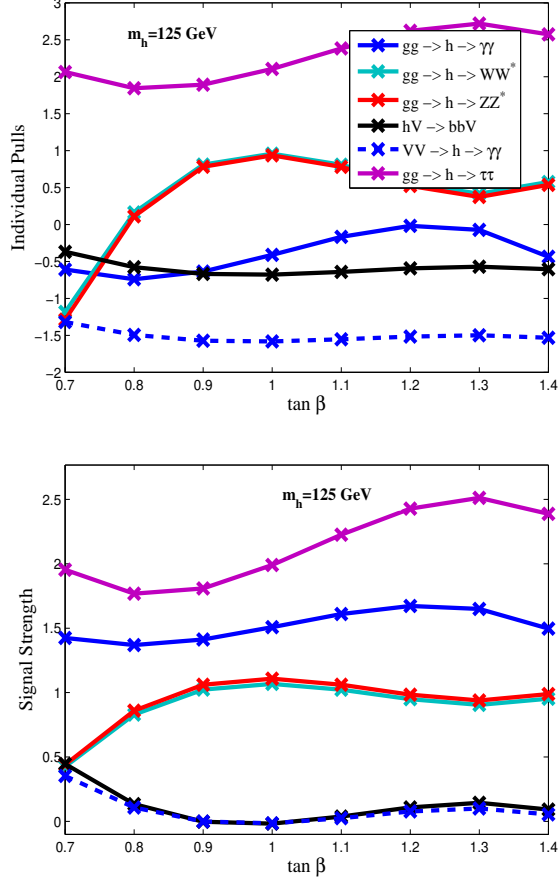


FIG. 6: The individual pulls $\frac{(R_{XX}^{Model} - R_{XX}^{Obs})}{\sigma_{XX}}$ (upper plot), and the signal strengths R_{XX}^{Model} (lower plot), in the different channels, that correspond to the best fitted 4G2HDM curve with $m_h = 125$ GeV and $M_{AG} = 400$ GeV, shown in Fig. 4.

comparing the calculated signal strengths:

$$R_{ZZ/WW}^H \equiv \frac{\sigma(pp \rightarrow H \rightarrow ZZ/WW)_{4G2HDM}}{\sigma(pp \rightarrow H \rightarrow ZZ/WW)_{SM}}, \quad (11)$$

to the observed/measured values of this quantity, i.e., to $R_{ZZ/WW}^{Obs}$ (note that in the 4G2HDM we find $R_{WW}^H \sim R_{ZZ}^H$ for $m_H > 2m_W$). In Fig. 7 we plot R_{ZZ}^H as a function of m_H for the 6 best fitted points of the relevant 4G2HDM parameter space, given in Table I. We also show in Fig. 7 an approximate exclusion line for R_{ZZ} , i.e., for the observed signal strength R_{ZZ}^{Obs} , which we have extracted from the most recent CMS exclusion plot in this channel (see [56]) and which is currently the most stringent observed exclusion limit for a heavy Higgs with a mass $\gtrsim 200$ GeV. We see that $m_H \lesssim 600$ GeV is excluded by the current data in the $H \rightarrow ZZ$ channel for points P1, P2, P3 and P5 (i.e., $R_{ZZ}^H(P1, P2, P3, P5) > R_{ZZ}^{Obs}$ for $m_H \lesssim 600$ GeV), while for point P4 and P6 $m_H \gtrsim 500$ GeV is allowed.

The current CMS and ATLAS Higgs data in the ZZ and WW channels are not sensitive to the pseudoscalar

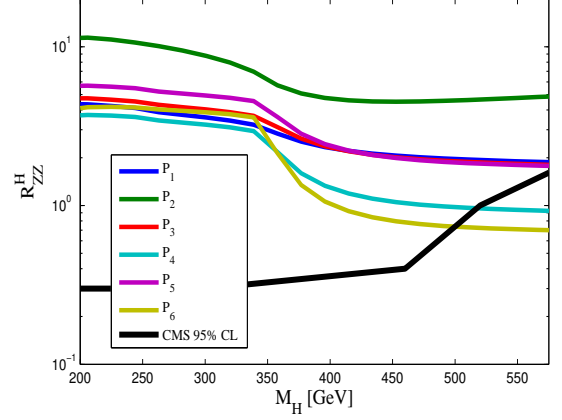


FIG. 7: The signal strength in the $H \rightarrow ZZ$ channel, for the 6 best fitted sets of values in Table I. Also shown is the approximate observed CMS limit on the signal strength in the ZZ channel, i.e., R_{ZZ}^{Obs} , see also text.

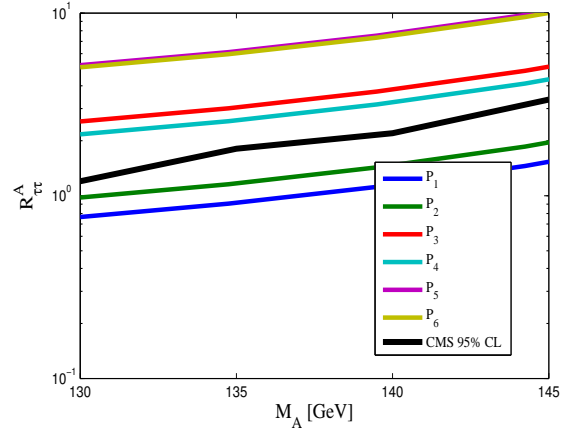


FIG. 8: The signal strengths in the $A \rightarrow \tau\tau$ channel, for the 6 best fitted sets of values in Table I. Also shown is the approximate observed CMS limit on signal strengths in the $\tau\tau$ channel, i.e., $R_{\tau\tau}^{Obs}$, see also text.

A , due to the absence of a tree level AZZ and AWW coupling (and due to the smallness of the corresponding AZZ and AWW one-loop couplings [57]). Therefore, the only relevant search channels which are currently sensitive to the A decays are $A \rightarrow \gamma\gamma$ and $A \rightarrow \tau\tau$, for which a search for the Higgs was performed up to a Higgs mass slightly below $2m_W$ by both CMS and ATLAS. Defining the signal strengths for the A signals as:

$$R_{\tau\tau/\gamma\gamma}^A \equiv \frac{\sigma(pp \rightarrow A \rightarrow \tau\tau/\gamma\gamma)_{4G2HDM}}{\sigma(pp \rightarrow H \rightarrow \tau\tau/\gamma\gamma)_{SM}}, \quad (12)$$

we plot in Figs. 8 and 9 $R_{\tau\tau}^A$ and $R_{\gamma\gamma}^A$, respectively, as a function of m_A (we assume that $m_A > m_h$), for points P1-P6 of Table I. Here also, we plot the existing approximate exclusion lines $R_{\tau\tau}^{Obs}$ and $R_{\gamma\gamma}^{Obs}$, based on the most recent CMS analysis, which currently gives the most

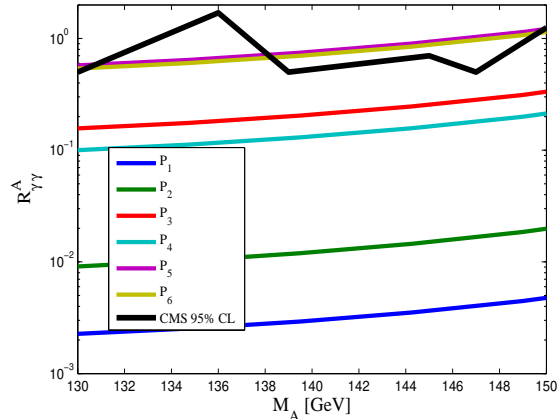


FIG. 9: The signal strengths in the $A \rightarrow \gamma\gamma$ channel, for the 6 best fitted sets of values in Table I. Also shown is the approximate observed CMS limit on signal strengths in the $\gamma\gamma$ channel, i.e., $R_{\gamma\gamma}^{Obs}$, see also text.

stringent limits in these two channels [58, 59]. We see that a pseudoscalar as light as 130 GeV is allowed by the current data, e.g., for for points P1 and P2.

V. SUMMARY

We have studied the recently measured Higgs signals in the framework of a specific 2HDM with a fourth generation of fermions (the 4G2HDM suggested in [33]), designed and motivated by the possibility that the sub-TeV Higgs particles are condensates of the heavy 4th generation fermions, which are therefore, viewed as the agents

of dynamical electroweak symmetry breaking.

We find that the lightest CP-even Higgs state of this model, h , is a good candidate for the recently discovered 125 GeV Higgs signals in all the measured channels, within a large portion of the 4G2HDM allowed parameter space, which is consistent with the current bounds from EWPD. In particular, for typical 4th generation fermion masses in the range $M_{4G} = 400 - 600$ GeV, $\tan\beta \sim \mathcal{O}(1)$ and a large $t - t'$ mixing (the parameter ϵ_t predicted by the model), the lightest 4G2HDM Higgs gives a good overall fit to the current 125 GeV Higgs data - roughly comparable to the SM fit.

For these values of the 4G2HDM parameter space, in particular with $\epsilon_t \sim 0.5$, the flavor changing t' decay $t' \rightarrow th$ dominates with $\text{BR}(t' \rightarrow th) \sim 1$, leading to different $pp \rightarrow t'\bar{t}'$ signatures (than the simple SM4) that can be searched for at the LHC using the methods suggested in [52].

We also find that, based on the current Higgs data, the 4G2HDM predicts large deviations from the SM in the channels $pp \rightarrow h \rightarrow \tau\tau$, $VV \rightarrow h \rightarrow \gamma\gamma$ and $hV \rightarrow Vbb$, which remains to be tested with more data.

Finally, the heavier CP-even Higgs state, H , is found to be excluded in this model up to ~ 500 GeV, while the pseudoscalar Higgs state, A , can be as light as 130 GeV and can, therefore, be discovered (or ruled out in this small mass range) with more data collected in the $pp \rightarrow \tau\tau, \gamma\gamma$ channels.

Acknowledgments: SBS and MG acknowledge research support from the Technion. GE thanks R. Godbole and S. Vempati for hospitality and discussions. The work of AS was supported in part by the U.S. DOE contract #DE-AC02-98CH10886(BNL).

-
- [1] S. Chatrchyan *et al.*, [CMS Collaboration], Phys. Lett. **B716**, 30 (2012); See also, J. Incandela, “Observation of a narrow resonance near 125 GeV in CMS”, talk given at the ICHEP 2012, July 4-11th, Melbourne, Australia.
- [2] G. Aad *et al.*, [ATLAS Collaboration], Phys. Lett. **B716**, 1 (2012); See also, R. Hawkings, “ATLAS Higgs searches and experiment overview”, talk given at the ICHEP 2012, July 4-11th, Melbourne, Australia.
- [3] [TEVNPH (Tevatron New Phenomena and Higgs Working Group) and CDF and D0 Collaborations], arXiv:1203.3774 [hep-ex].
- [4] P.H. Frampton, P.Q. Hung and M. Sher, Phys. Rept. **330**, 263 (2000).
- [5] B. Holdom, W.S. Hou, T. Hurth, M.L. Mangano, S. Sultanoy, G. Unel, talk presented at *Beyond the 3rd SM generation at the LHC era workshop*, Geneva, Switzerland, Sep 2008, arXiv:0904.4698 [hep-ph], published in PMC Phys. **A3**, 4 (2009).
- [6] For older literature on the SM4, see: Proceedings of the First (February 1987) and the Second (February 1989) International Symposiums on the *fourth family of quarks and leptons*, Santa Monica, CA, published in Annals of the New York Academy of Sciences, 517 (1987) & 578 (1989), edited by D. Cline and A. Soni.
- [7] For a review of the implications of stable quarks of the 4th generation on cosmology, astrophysics and accelerator physics, see: K. Belotsky, M. Khlopov and K. Shibaev, arXiv:0806.1067 [astro-ph] and references therein.
- [8] B. Holdom, Phys. Rev. Lett. **57**, 2496 (1986), Erratum-ibid. **58**, 177 (1987); W.A. Bardeen, C.T. Hill and M. Lindner, Phys. Rev. **D41**, 1647 (1990); S.F. King, Phys. Lett. **B234**, 108 (1990); C. Hill, M. Luty and E.A. Paschos, Phys. Rev. **D43**, 3011 (1991); P.Q. Hung and G. Isidori Phys. Lett. **B402**, 122 (1997).
- [9] B. Holdom, JHEP **0608**, 76 (2006).
- [10] P.Q. Hung, Chi Xiong, Nucl.Phys. **B848**, 288 (2011).
- [11] Y. Mimura, W.S. Hou and H Kohyama, arXiv:1206.6063 [hep-ph].
- [12] W.S. Hou, Chin. J. Phys. **47**, 134 (2009); W.S. Hou, talk given at the *34th International Conference on High Energy Physics (ICHEP 2008)*, Philadelphia, Pennsylvania, July 2008, arXiv:0810.3396 [hep-ph]; S.W. Ham, S.K. Oh, D. Son, Phys. Rev. **D71**, 015001 (2005); G. W.S. Hou, Int. J. Mod. Phys. **D20**, 1521 (2011).

- [13] S.W. Ham, S.K. Oh, D. Son, Phys. Rev. **D71**, 015001 (2005); R. Fok, G.D. Kribs, Phys. Rev. **D78**, 075023 (2008).
- [14] A. Soni, A. K. Alok, A. Giri, R. Mohanta and S. Nandi, Phys. Lett. **B683**, 302 (2010).
- [15] A. Soni, A. K. Alok, A. Giri, R. Mohanta and S. Nandi, Phys. Rev. **D82**, 033009 (2010).
- [16] A. J. Buras, B. Duling, T. Feldmann, T. Heidsieck, C. Promberger and S. Recksiegel, JHEP **1009**, 106 (2010).
- [17] A. J. Buras, B. Duling, T. Feldmann, T. Heidsieck, C. Promberger and S. Recksiegel, JHEP **1007**, 094 (2010).
- [18] W.-S. Hou, M. Nagashima, A. Soddu, Phys. Rev. **D76**, 016004 (2007); M. Bobrowski, A. Lenz, J. Riedl and J. Rohrwild, Phys. Rev. **D79**, 113006 (2009); V. Bashiry, N. Shirkhanghah, K. Zeynali, Phys. Rev. **D80**, 015016 (2009); W. S. Hou and C. Y. Ma, Phys. Rev. **D82**, 036002 (2010); O. Eberhardt, A. Lenz and J. Rohrwild, Phys. Rev. **D82**, 095006 (2010); S. Nandi and A. Soni, Phys. Rev. **D83**, 114510 (2011); A.K. Alok, A. Dighe and D. London, Phys. Rev. **D83**, 073008 (2011) 073008; D. Choudhury, D. K. Ghosh, JHEP **1102**, 033 (2011); R. Mohanta, A.K. Giri, Phys. Rev. **D85**, 014008 (2012); A. Ahmed, I. Ahmed, M.J. Aslam, M. Junaid, M.A. Paracha, A. Rehman, Phys. Rev. **D85**, 034018 (2012).
- [19] The Review of Particle Physics, K. Nakamura *et al.* [Particle Data Group], J. Phys. **G37**, 075021 (2010).
- [20] M.M.H. Luk [on behalf of the CMS Collaboration], arXiv:1110.3246v2 [hep-ex]; S. Chatrchyan *et al.* [CMS Collaboration], Phys. Lett. **B716**, 103 (2012); G. Aad *et al.* [ATLAS Collaboration], Phys. Rev. Lett. **109**, 032001 (2012); S. Chatrchyan *et al.* [CMS Collaboration], JHEP **1205**, 123 (2012).
- [21] The ATLAS Collaboration, note: ATLAS Conference note 2011-135; S. Chatrchyan *et al.* [CMS Collaboration], Phys. Lett. **B710**, 26 (2012).
- [22] O. Eberhardt *et al.*, Phys. Rev. **D86**, 013011 (2012).
- [23] A. Djouadi and A. Lenz, Phys. Lett. **B715**, 310 (2012).
- [24] E. Kuflik, Y. Nir and T. Volanski, arXiv:1204.1975 [hep-ph].
- [25] O. Eberhardt, A. Lenz, A. Menzel, U. Nierste, M. Wiebusch, arXiv:1207.0438 [hep-ph].
- [26] G. D. Kribs, T. Plehn, M. Spannowsky and T. M. P. Tait, Phys. Rev. **D76**, 075016 (2007).
- [27] G. Passarino, C. Sturm and S. Uccirati, Phys. Lett. **B706** 195-199 (2012).
- [28] A. Denner *et al.*, Eur. Phys. J. **C72**, 1992 (2012).
- [29] G. Guo, B. Ren and X.-G. He, arXiv:1112.3188 [hep-ph].
- [30] O. Eberhardt *et al.*, arXiv:1209.1101 [hep-ph].
- [31] M.A. Luty, Phys. Rev. **D41**, 2893 (1990).
- [32] M. Hashimoto and V.A. Miransky, Phys. Rev. **D81**, 055014 (2010).
- [33] S. Bar-Shalom, S. Nandi and A. Soni, Phys. Rev. **D84**, 053009 (2011).
- [34] P.Q. Hung, C. Xiong, Nucl. Phys. **B847**, 160 (2011).
- [35] P.Q. Hung, C. Xiong, Phys. Lett. **B694**, 430 (2011).
- [36] K. Ishiwata and M.B. Wise, Phys. Rev. **D83**, 074015 (2011).
- [37] A.E.C. Hernandez, C.O. Dib, H.N. Neill and A.R. Zerwekh, JHEP **1202**, 132 (2012).
- [38] G. Burdman and L. Da Rold, JHEP **0712**, 86 (2007).
- [39] G. Burdman, L. Da Rold, O. Eboli and R.D. Matheus, Phys. Rev. **D79**, 075026 (2009); G. Burdman, L. de Lima and R.D. Matheus, Phys. Rev. **D83**, 035012 (2011).
- [40] E. De Pree, G. Marshall and M. Sher, Phys. Rev. **D80**, 037301 (2009).
- [41] H.-S. Lee and A. Soni, arXiv:1206.6110 [hep-ph].
- [42] M. Sher, Phys. Rev. **D61**, 057303 (2000).
- [43] W. Bernreuther, P. Gonzales and M. Wiebusch, Eur. Phys. J. **C69**, 31 (2010).
- [44] John F. Gunion, arXiv:1105.3965 [hep-ph].
- [45] G. Burdman, C. Haluch and R. Matheus, JHEP **1112**, 038 (2011).
- [46] X.-G. He and G. Valencia, Phys. Lett. **B707**, 381 (2012).
- [47] N. Chen and H. He, JHEP **1204**, 062 (2012).
- [48] S. Litsey, M. Sher, Phys. Rev. **D80**, 057701 (2009).
- [49] S. Dawson, P. Jaiswal, Phys. Rev. **D82**, 073017 (2010).
- [50] R.C. Cotta, J.L. Hewett, A. Ismail, M.-P. Le and T.G. Rizzo, Phys. Rev. **D84**, 075019 (2011).
- [51] S. Bar-Shalom, M. Geller, S. Nandi and A. Soni, arXiv:1208.3195 [hep-ph], a review to appear in a special issue of Advances in High Energy Physics (AHEP) on Very Heavy Quarks at the LHC.
- [52] M. Geller, S. Bar-Shalom and G. Eilam, Phys. Lett. **B715**, 121 (2012).
- [53] J. Campbell, "Perturbative QCD Status", talk given at ICHEP 2012, Melbourne.
- [54] A. Djouadi, J. Kalinowski and M. Spira, Comput. Phys. Commun. **108**, 56 (1998), with contributions from arXiv:hep-ph/9704448 [hep-ph].
- [55] L. Bellantoni, J. Erler, J. Heckman and E. Ramirez-Homs, Phys. Rev. **D86**, 034022 (2012).
- [56] The CMS collaboration, CMS Physics Analysis Summaries, Report Number: CMS-PAS-HIG-12-016, available on the CERN CDS information server.
- [57] See e.g., J.F. Gunion, H.E. Haber and C. Kao, Phys. Rev. **D46**, 2907 (1992).
- [58] The CMS collaboration, CMS Physics Analysis Summaries, Report Number: CMS-PAS-HIG-12-018, available on the CERN CDS information server.
- [59] The CMS collaboration, CMS Physics Analysis Summaries, Report Number: CMS-PAS-HIG-12-015, available on the CERN CDS information server.